XVII IMEKO World Congress
Metrology in the 3rd Millennium
June 22-27, 2003, Dubrovnik, Croatia

DISTANCE MEASUREMENTS WITH LASER-TRIANGULATION IN HOT ENVIRONMENTS

Dirk Stöbener, Matko Dijkman, Dennis Kruse, Holger Surm, Olaf Keßler*, Peter Mayr*, Gert Goch*

University of Bremen, Department of Production Engineering, Bremen, Germany
* Institute for Material Science (IWT), Bremen, Germany

Abstract – Tactile distance measurement systems with uncertainties in the micrometer range cannot be used in hot environments with temperatures above 800 °C. A green laser-triangulation system with appropriate optical filters can meet these requirements. A measuring system was build up and tested at room temperature and in two different heat treatment furnaces at temperatures up to 900 °C. Good linearity of the system and acceptable correspondence between measurements and published reference values could be observed. The results show the suitability of the system for distortion measurements in heat treatment furnaces.

Keywords: laser-triangulation, position measurement, high temperature.

1. INTRODUCTION

The production process of heavily loaded metal parts is usually finished by heat treatment in order to achieve the desired properties of the material. Each step of the complete production process induces different distortion potentials in the workpiece. During the heat treatment, these induced potentials lead to distortion of the workpiece, which means that undesired changes in size and shape of the piece occur. Hence, a follow-up treatment (i.e. grinding) is often necessary to reach the tolerance range of the workpiece.

Due to the high costs of the follow-up manufacturing step an intense industrial interest exists in solutions, which help to understand and control the effects of distortion. Recent investigations concentrated on single production processes and cannot be used for a general understanding of distortion phenomena [1-4].

The collaborative research centre 570 (SFB570) of the Deutsche Forschungsgemeinschaft (DFG) investigates each single step of the production chain in order to understand its contributions to distortion effects for representative workpieces.

Thus, changes in size and shape of the workpiece have to be measured, even during the heat treatment. The size changes due to thermal expansion and transformations span a range of several mm. The changes due to induced distortion potentials are assumed to be in the range of some tenth mm. Hence, the measuring uncertainty of displacement should reach 20 µm or less.

The biggest problem for measurements is the high temperature in the heat treatment furnace, which reaches up

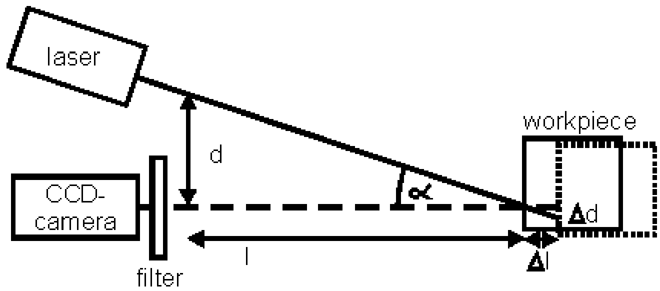

Fig. 1: Experimental setup of the laser-triangul. system without PC

to 950° C. Tactile measuring systems cannot be used in this hot environment without being damaged or affecting the surface of the workpiece.

Reference [5] describes a measuring system based on capacitive effects, which is used for non-tactile distance measurements in a furnace with temperatures of about 900° C. The uncertainty of this system is specified as 2,5 mm on a maximum distance of 60 mm. Another solution for environment temperatures exceeding 1200° C is described in [6]. The authors estimate the uncertainty of the system as 1 cm on a measuring range of 20 m.

Both systems are not useful for distortion measurements during heat treatment, because they do not meet the requirements mentioned above concerning measuring range and uncertainty.

A laser-triangulation system can fulfil these requirements. Depending on the technical setup and the measuring range, uncertainties better than 1 µm can be reached in industrial systems [7]. The high temperature in the furnace requires a safety distance between measurement system and furnace to prevent system damage. Due to the non-tactile principle of the laser-triangulation system, measurement distances up to metres are achievable.

2. THEORY AND SETUP

2.1. Laser-triangulation: principle of operation

The laser-triangulation system consists of a laser, an optical filter, a CCD-camera with a lens system and a PC including a framegrabber and an evaluation software (fig.1). With the known distances d and l between the measuring object, the camera and the laser source, the angle a can be calculated. The change of the workpiece position Δl leads to a change Δd of the laser-spot position on the surface. The laser-spot is observed by the camera and the evaluation software determines the position of the spot centre. The factor *ß* describes the relationship between the change of centre position Δp in the image and the spot position change Δd on the workpiece surface:

$$\Delta d = b \cdot \Delta p \quad (1)$$

The displacement of the front surface Δl is then calculated by (2):

$$\Delta l = \frac{\Delta d}{\tan a} = b \cdot \frac{\Delta p}{\tan a} \quad (2)$$

2.2. Theoretical intensity estimation

Optical measurements of workpieces at red heat may cause difficulties in detecting the laser spot. A small uncertainty in the determination of the spot centre can only be guaranteed, if a sufficient contrast between laser reflection and workpiece emission exists. In order to choose an appropriate laser wavelength and a suitable filter, the emitted power P of a unit area of the workpiece is estimated by Planck's law [8]

$$P = \int \frac{2phn^3}{c^2} \cdot \frac{1}{\exp\left(hu/kT\right) - 1} du \quad (3)$$

and the result is compared with the radiation power of the laser (h: Planck's constant, k: Boltzmann's constant, T: temperature, n: light frequency, c: light velocity).

The wavelength-depending sensitivity of the camera limits the wavelength region, which has to be taken into account for the estimation of the emitted power of the workpiece. The used camera covers the bandwidth between 2,0 µm and 350 nm.

Within this wavelength region, the result of the exponential function in (3) exceeds the value 1 by far:

$$\exp\left(\frac{hu}{kT}\right) >> 1 \Rightarrow \frac{1}{\exp\left(hu/kT\right) - 1} \approx \exp\left(-\frac{hu}{kT}\right). \quad (4)$$

Hence, Planck's law can be approximated by the following formula:

$$P \approx \frac{2ph}{c^2} \int u^3 \cdot \exp\left(-\frac{hu}{kT}\right) du \ . \quad (5)$$

The integration of this formula between the limits ν_1 and ν_2 yields the emitted power values listed in table I.

TABLE I: Estimated emitted powers for different wavelengths λ

Limits $\lambda_{1,2}$ in nm	Power in Watt/m^2
1000-2000 (infrared)	> 15000
570-1000 (red + infrared)	~ 250
350-570 (green + blue)	< 0,25

If a coefficient of smaller than 0,5 for the laser light reflection on the workpiece (spot-diameter ≈ 1 mm) towards the camera is assumed, table I shows that the reflected light of a red laser (1 mW/mm^2) has almost the same power as the emission of the workpiece on an area of 1 mm^2. Therefore, the red laser-spot cannot be clearly observed in the image. The emitted intensity in the green region is much smaller. Hence, the system was build up with a green Ar^+-Laser (15 mW) and a blue glass filter in front of the camera with high transmission rates below 550 nm, to block the red and infrared emission from the workpiece. As a result, a high contrast between laser-spot and workpiece is achieved, which allows a clear detection of the spot.

2.3. Experimental setup 1

The experimental setup 1 consists of the above-mentioned green Ar^+-Laser completed with the other parts shown in fig. 1 (and mentioned in section 2.1), a cuboid workpiece and a furnace, which is based on the resistance heating principle. The workpiece is placed in the furnace and the laser-triangulation system points towards it from outside the furnace.

2.4. Experimental setup 2

The second setup includes mainly the same parts as the first. An induction furnace with a cylindrical workpiece with diameter 50 mm replaces the resistance-heating furnace [9]. The samples were prepared using bearing steel AISI 52100. The laser system points through the coils of the inductive heating element on the workpiece and the camera observes the laser-spot through these coils as well. The advantage of this setup is the defined fixture of the heated sample, so that surface position movements can directly be correlated to thermal expansion and transformations. Further, these samples were equipped with thermocouples.

3. RESULTS

Fig. 2 presents the result of the first test of the laser system in experimental setup 1. The furnace was heated to a temperature of 1100 °C and the laser pointed on the workpiece. The left part (A) of fig. 2 shows an image taken by the camera without the filter in front of it. The furnace and a part of the workpiece inside are visible. It is not possible to identify the laser-spot due to high red and infrared emission of the furnace and the workpiece. In

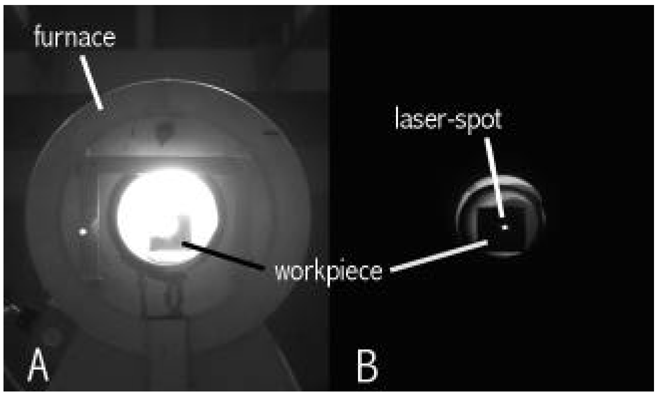

Fig. 2: Image of the furnace without (A) and with (B) optical filter in front of the camera

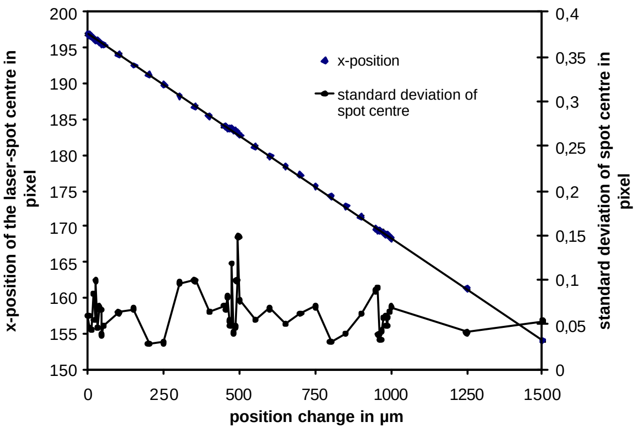

Fig. 3: Comparison between laser-triangulation and reference gauge

part B the image taken with the filter in front of the camera is shown. The filter blocks most of the emitted red and infrared radiation. Thus, only the hot background of the furnace, the whole workpiece and the laser-spot are clearly recognizable, which is in good agreement with the theoretical intensity estimation in section 2.2..

Other measurements with setup 1 were carried out in the cold furnace at room temperature to test the linearity of the system. The workpiece was moved with a micrometer drive. The comparison between the calculated results of the laser-spot centre and the values of a reference gauge (fig. 3) shows good linearity.

Each workpiece position was measured 20 times with the laser-triangulation system. Its standard deviation σ, shown on the right scale in fig. 3, was calculated with (6) for each measurement position. It is smaller than 0,2 pixel of the laser-spot image, which corresponds to approximately 6 µm for each position.

$$s = \sqrt{\frac{\sum_{i=1}^{n} (x_i - \bar{x})^2}{n-1}} \quad (6)$$

For a first test of the system uncertainty at higher temperatures, the cuboid workpiece was placed in the furnace of setup 1. Its fixed surface position was measured 50 times each at four different temperatures T (Table II).

TABLE II: Standard deviations σ of laser-spot centre for different temperatures

T in °C	σ in pixel	T in °C	σ in pixel
620	0,41 (~ 14 µm)	800	0,53 (~ 19 µm)
710	0,45 (~ 16 µm)	875	0,53 (~ 19 µm)

The standard deviation doesn't increase above 20 µm, even for temperatures up to 875 °C. Accordingly, the system should be suitable for distortion measurements during heat treatment. To further test the suitability, other measurements were carried out with experimental setup 2.

The induction furnace allows a more precise heating of the cylindrical workpiece than the resistance furnace in

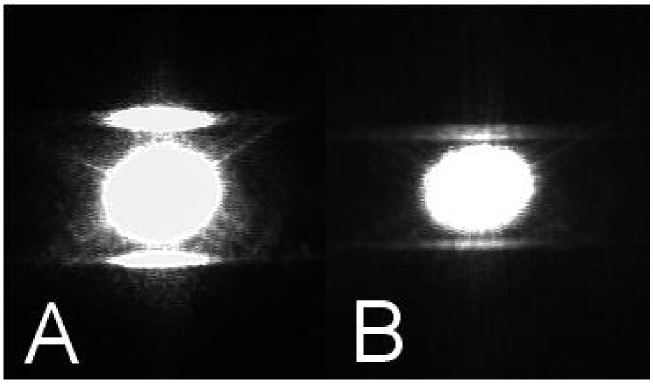

Fig. 4: Laser-spot reflection without (A) and with (B) blackened induction coils

setup 1. The workpiece is mounted with its centre to a holder, which itself is fixed to the furnace wall. Therefore, the workpiece expands symmetrically in all radial directions when it is heated.

As described in section 2.4. the laser points through the gap between the coils (about 1-2 mm) of the inductive heating element. Due to the small gap, undesired reflections of the laser-spot can occur. They are suppressed by blackening the coils with paint. The left part (A) of fig. 4 shows the reflection of the laser-spot with untreated coils and the right part (B) with blackened coils. An estimation of the laser-spot position with an appropriate uncertainty is only possible with blackened coils.

The calibration for the relationship between x-position of the laser-spot centre and the position change of the workpiece surface yields a factor of 60,5 µm per pixel for setup 2. The calibration was performed in the same way as the linearity measurement for setup 1, which is shown in fig. 3.

Fig. 5 presents the results of the first measurements with setup 2. In addition to the expansion, also the temperature of the workpiece was measured with thermocouples. The correlation between the temperature and the expansion is satisfying. During heating some irregularities ("waves") can be observed in the expansion curve. They probably result from vibrations or small, undefined movements of the holder in the furnace due to its expansion.

For a comparison of the results with a reference method,

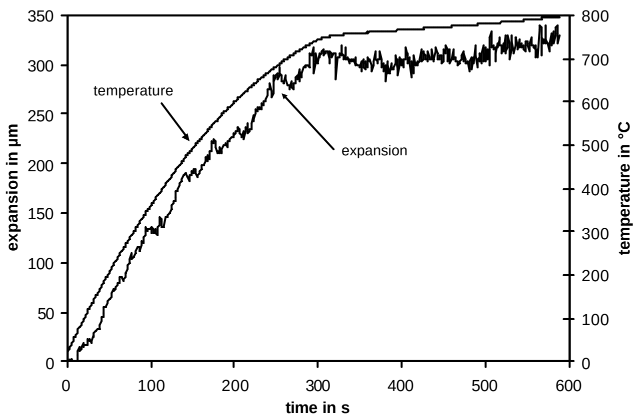

Fig. 5: Time dependent expansion d and temperature T of the workpiece

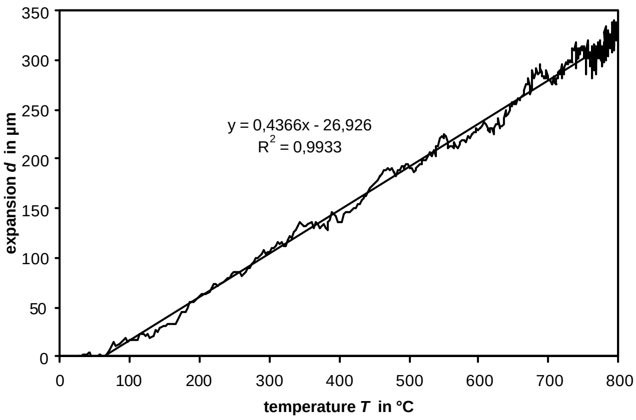

Fig. 6: Expansion d as function of temperature T

the measured values (expansion d, temperature T) are plotted as a linear function of each other (fig. 6). The slope of the curve divided by the workpiece radius gives the expansion coefficient a_l, which can be compared to a value published in [10,11]. Table III lists both values.

TABLE III: Expansion coefficient a_l of steel AISI 52100:

	laser-triangulation	comparative value [10,11]
a_l in 1/°C $*10^{-6}$	18,6	15 ± 1

The calculated expansion coefficient is 24% higher than the published comparative value. A possible explanation of this discrepancy is a deviation in the calculation of the expansion coefficient due to wrong temperature values. The temperature measurement in the workpiece involves two thermo couples. The first one is positioned 3 mm behind the observed surface. The second thermocouple is placed in the middle between the surface and the centre of the workpiece. The inductive element only heats the surface of the workpiece and a small area beneath it. The volume of the workpiece warms up by heat conduction. To overcome this problem, low induction heating powers were used in order to achieve only a small temperature gradient in the workpiece. Nevertheless, the temperature measurements of the two thermocouples show different values during the experiment. The difference reaches values up to 30 °C. Hence, the mean value of both elements is only an approximation of the temperature.

Dilatometer measurements can also be used as a reference for the results obtained with the laser-triangulation system. Again, temperature and expansion values were recorded with the triangulation system for steel 52100 at a defined heating rate.

Another workpiece of steel 52100 was examined in a dilatometer. The dilatometer experiments were carried out in a quenching- and deformation dilatometer DIL 805A/D from Bähr Thermoanalyse. This dilatometer is used for the determination of continuous and isothermal TTT- diagrams [12]. High heating rates of up to 4000 K/s and cooling rates of 2500 K/s are the main features.

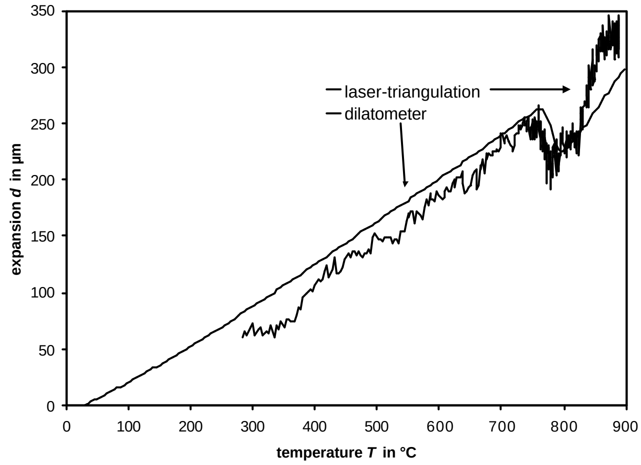

Fig. 7: Comparison between laser-triangulation and dilatometer measurements

Heating is realized by induction. Samples of ø 4 mm and 10 mm length are used. During austenitizing, a vacuum of $8x10^{-3}$ mbar is established. Quenching can be realized in a gas nozzle field with nitrogen or helium. A processor system records temperature, time, and length change.

In the dilatometer and the laser-triangulation experiment the heating rate was approximately 3 K/s.

The results of both measurements are presented in fig. 7. Both curves are close to each other and show the same characteristics. Even the volume change during the austenitizing above 765 °C is clearly observable in the laser-triangulation measurement. This similarity between both curves is another proof for the suitability of the laser-triangulation system.

The offset for lower temperatures is inevitable, because the laser-triangulation system started to measure at a different temperature as the dilatometer. This corresponds to an unknown expansion offset for the laser-triangulation results. No explanation for the difference between both measurements above 830 °C was found, as yet.

Besides the above-described measurements, also uncertainty examinations were carried out for setup 2. Depending on the chosen heating rate for the inductive heating, only a definite maximum temperature is reachable. Just a small increase of temperature per time unit remains, if this temperature range is attained. This fact is used for repeatability experiments. Fig. 8 presents the results for an almost constant temperature of 740 °C. The plot for the scale on the left side shows the measured expansion d and a least square fit line. The plot for the right scale shows the difference between the approximated straight and the measured values. This difference represents an estimate of the repeatability of the measurements at 740 °C. The values range from –20 to 20 µm. The standard deviation of these differences is 8,5 µm. This is below the value estimated with setup 1 and also below the requirements stated in section 1.

4. CONCLUSIONS

The application of a laser-optical system for distortion measurements in a heat treatment furnace shows promising results. The presence of light emission (infrared and red) of

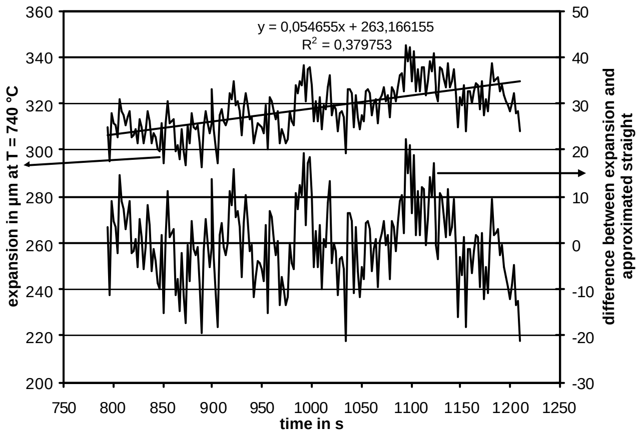

Fig. 8: Expansion measurements at almost constant temperature

the workpiece does not effect the detection of the laser-light, if a green laser and a suitable filter in front of the camera are used. The system was tested using steel AISI 52100 samples. Comparisons of the measured values with comparative values from literature or dilatometer measurements showed good agreement. Even the volume change during the transformation of ferrite to austenite can be detected. First experiments lead to a repeatability of less than 10 µm for displacements measurements at high temperature. Hence, a measuring uncertainty better than 20 µm appears reachable, fulfilling the requirements of distortion measurements. Further investigations regarding the uncertainty and detection limit are planned.

A major restriction of the laser-triangulation system is the fact that measurement information only exists for one point. This cannot describe the changes of size and shape of the workpiece sufficiently. Further development will aim at a laser-light-slit system based on laser-triangulation, which obtains information about a line (not only a point) of the workpiece surface. Furthermore, scanning mechanisms will be tested.

REFERENCES

[1] *Proc. 1st International Conference on Quenching and the Control of Distortion, sept. 22.-25.,* Chicago, 1992

[2] *Proc. 2nd International Conference on Quenching and the Control of Distortion, nov. 4.-7.*, Cleveland, 1996

[3] S. Denis et al., “Prediction of residual stress and distortion of ferrous and non-ferrous metals: current and future developments”, *Proc. 3rd International Conference on Quenching and the Control of Distortion, march 24.-26., pp.* 263-276, Prag, 1999

[4] A. Thuvander, A. Germidis, “Numerical prediction of heat treatment distortion of HSS-Importance of proeutectoid carbides”, *Proc. 3rd International Conference on Quenching and the Control of Distortion, march 24.-26., pp. 311-321,* Prag, 1999

[5] A. Dumbs, E. Bergmann, „Entwicklung eines kapazitiven Sensorsystems für Hochtemperaturanlagen“, *Forschungsbericht HA 84-027 des Bundesministeriums für Forschung und Technologie*, 1984

[6] K. Määttä, J. Kostamovaara, R. Myllylä, „A laser rangefinder for hot surface profiling measurements“, *SPIE Vol. 952 Laser Technologies in Industry*, pp. 356-364, 1988

[7] „Kompetenz in Wegmessung“, *Produktübersicht 2002*, Micro-Epsilon, 2002

[8] H. Kuchling, „Taschenbuch der Physik“, 13. Auflage, Fachbuchverlag GmbH, Leipzig, 1991

[9] K. Pantleon, O. Keßler, F. Hoffmann, P. Mayr, “Induction surface hardening of hard coated steels”, *Surface and Coatings Technology*, 120-121 (1999), 495-501

[10] „Physikalische Eigenschaften von Stählen“, *Stahl-Eisen-Werkstoffblätter (SEW) 310*, 1. Ausgabe, Verlag Stahleisen mbH, 1992

[11] F. Richter, „Physikalische Eigenschaften von Stählen und ihre Temperaturabhängigkeit“, *Stahleisen-Sonderberichte, Heft 10,* Verlag Stahleisen mbH, Düsseldorf, 1983

[12] „Atlas zur Wärmebehandlung der Stähle“, Max-Planck-Institut für Eisenforschung, Band I-IV, Verlag Stahleisen mbH, Düsseldorf

Authors:
Dirk Stöbener, University of Bremen, Department of Measurement and Control (MSR), Faculty of Production Engineering, Badgasteiner Str. 1, 28359 Bremen, Germany, phone: +49-421-218-5483, fax: +49-421-218-4220, d.stoebener@msr.uni-bremen.de,
Matko Dijkman, University address: see above, phone: +49-421-218-2334, fax: +49-421-218-4220, m.dijkman@msr.uni-bremen.de,
Dennis Kruse, University address: see above, phone: +49-421-218-2334, fax: +49-421-218-4220, kru@biba.uni-bremen.de,
Prof. Dr.-Ing. Gert Goch, University address: see above, phone: +49-421-218-5515, fax: +49-421-218-5625, gg@biba.uni-bremen.de
Holger Surm, Institute for Material Science (IWT), Badgasteiner Str. 3, 28359 Bremen, Germany, phone: +49-421-218-5342, fax: +49-421-218-5333, surm@iwt-bremen.de,
Dr.-Ing. Olaf Keßler, IWT address: see above, phone: +49-421-218-5325, fax: +49-421-218-5333, kessler@iwt-bremen.de,
Prof. Dr.-Ing. habil. Peter Mayr, IWT address: see above, phone: +49-421-218-5300, fax: +49-421-218-5474, mayr@iwt-bremen.de

ACKNOWLEDGEMENTS:

The authors wish to thank the DFG for funding the projects A5 and B3 in the collaborative research centre 570.